ChemComm

Conjugation *versus* rotation: good conjugation weakens the aggregation-induced emission effect of siloles†

Bin Chen,[a] Han Nie,[b] Ping Lu,[c] Jian Zhou,[a] Anjun Qin,[b] Huayu Qiu,[a] Zujin Zhao*[ab] and Ben Zhong Tang*[bd]

Incorporation of polycyclic aromatic hydrocarbons into siloles enhances their light emission in solutions but lowers emission efficiency in the aggregated state. The competitive interaction between conjugation and rotation is thus studied.

2,3,4,5-Tetraphenylsiloles (*e.g.* DMTPS and MPPS, Scheme 1) are interesting luminogens with aggregation-induced emission (AIE) characteristics.[1] They are almost nonfluorescent in solutions but become highly emissive in the aggregated state. The phenyl (Ph) rings at the 3,4-positions of silole rings are indispensable to make the molecules AIE-active, while the substituents at the 2,5-positions have a significant impact on the conjugation and emission color.[2,3] It has been rationalized that the intramolecular rotation (IMR) of Ph rotors against the silole ring stator deactivates the excited state of the molecule nonradiatively, which leads to weak emission in solutions.[4] But, normally, it is considered that a good conjugation between building blocks is favored for light emission. So, what will happen to silole's AIE characteristic when the molecular conjugation is extended? To address this issue, herein, a series of tailored siloles substituted with polycyclic aromatic hydrocarbons (PAH), naphthalene (Np) and anthracene (An), are designed and synthesized (Scheme 1 and Scheme S1, ESI†), based on the fact that PAHs can effectively prolong the
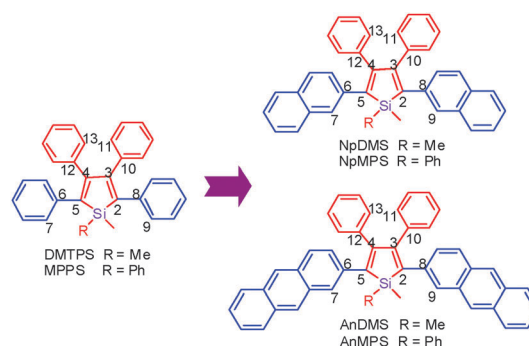
Scheme 1   Chemical structures of 2,3,4,5-tetraarylsiloles.

molecular conjugation without introducing more rotatable aromatic rings. The synthetic procedures and characterization data of new siloles are given in the ESI.† The photophysical properties are investigated and theoretical calculations are performed to reveal the structure–property relationship of new siloles.

The absorption spectra of new siloles in dilute THF solutions are shown in Fig. 1A. NpDMS shows an absorption maximum at 377 nm, associated with the π–π* transition of the molecule, which is red-shifted by 19 nm than that of DMTPS (Table 1). The absorption maximum of AnDMS is located at 415 nm, being 38 nm longer than that of NpDMS. A similar difference is also found by comparing the absorption maxima of MPPS (363 nm), NpMPS (382 nm) and AnMPS (420 nm). These results indicate that the conjugation of siloles is extended greatly by the incorporation of PAHs. Meanwhile, changing the 1,1-substituents from two methyls to one methyl and one Ph at the 1,1-positions of silole rings also moves the absorption spectra to the long-wavelength region due to the inductive effect.[2f] The photoluminescence (PL) properties of the siloles in solutions are improved after the substitution with PAHs. NpDMS and NpMPS emit at 505 and 508 nm, with fluorescence quantum yields (Φ_F) of 2.2 and 2.4%, respectively. The Φ_F values are low, but have increased notably relative to those of DMTPS (0.11%) and MPPS (0.09%).[5] AnDMS shows a main emission band peaked at 520 nm contributed

[a] *College of Material, Chemistry and Chemical Engineering, Hangzhou Normal University, Hangzhou 310036, China. E-mail: zujinzhao@gmail.com*
[b] *State Key Laboratory of Luminescent Materials and Devices, South China University of Technology, Guangzhou 510640, China*
[c] *State Key Laboratory of Supramolecular Structure and Materials, Jilin University, Changchun 130012, China*
[d] *Department of Chemistry, Institute for Advanced Study, Institute of Molecular Functional Materials, Division of Life Science, Division of Biomedical Engineering, and State Key Laboratory of Molecular Neuroscience, The Hong Kong University of Science & Technology, Clear Water Bay, Hong Kong, China. E-mail: tangbenz@ust.hk*
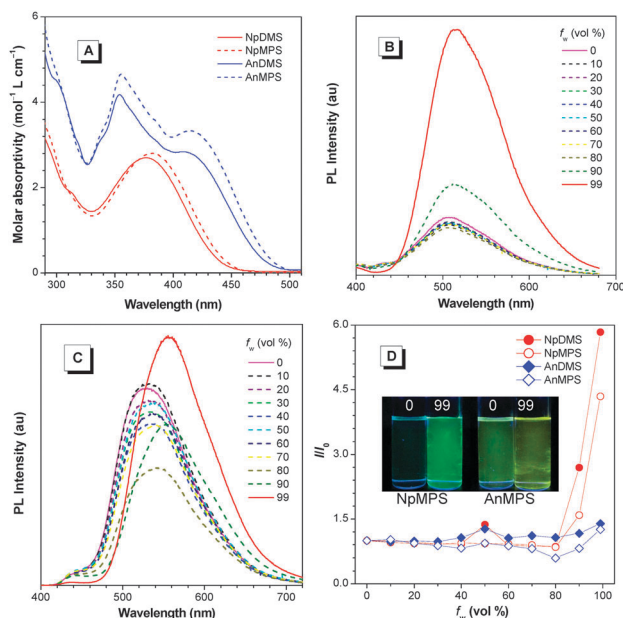
Fig. 1 (A) Absorption spectra of NpDMS, NpMPS, AnDMS and AnMPS in THF solutions. PL spectra of (B) NpMPS and (C) AnMPS in THF–water mixtures with different water fractions (f_w). (D) Plots of I/I_0 versus water fractions in THF–water mixtures, where I_0 is the PL intensity in pure THF solution. Inset: photos of NpMPS and AnMPS in THF–water mixtures ($f_w = 0$ and 99%), taken under the illumination of a UV lamp (365 nm).

Table 1 Optical properties of 2,3,4,5-tetraarylsiloles

	λ_{abs} (nm)	λ_{em} (nm) [Φ_F (%)]		
	Soln ($\varepsilon/10^4$)[a]	Soln[a]	Aggr[b]	Film[c]
DMTPS[d]	358 (0.88)	488 (0.11)	482 (22)	481 (76)
MPPS[d]	363 (0.81)	494 (0.09)	494 (22)	491 (85)
NpDMS	377 (2.7)	505 (2.2)	509 (16)	500 (48)
NpMPS	382 (2.6)	508 (2.4)	515 (15)	515 (37)
AnDMS	415 (2.8)	436, 520 (12)	546 (13)	533 (16)
AnMPS	420 (3.3)	444, 530 (11)	558 (13)	559 (14)

[a] In THF solution (10 μM); ε = molar absorptivity (mol^{-1} L cm^{-1}). [b] Aggregates formed in THF–water mixtures with a water fraction of 99% (vol%). [c] Film drop-casted on quartz plate. Fluorescence quantum yields in the solutions and aggregates, given in the parentheses, are determined using 9,10-diphenylanthracene (Φ_F = 90% in cyclohexane) as a standard, and those of the films are measured by the integrating sphere. [d] The data are cited from ref. 5.

mainly by π-extended silole rings. A weak shoulder at 436 nm is observed, which is largely due to the emission of An segments.[6] AnMPS shows the emission maximum at 530 nm, with a weak emission trace at 444 nm. The Φ_F values of AnDMS and AnMPS reach 12 and 11%, respectively, which are much higher than those of NpDMS and NpMPS. These results imply that incorporation of PAHs compensates emission quenching by the IMR process, particularly, the rotations of Phs at the 3,4-positions, and leads to a conspicuous emission enhancement in solutions.[7]

To study the emission behaviors of new siloles in the aggregated state, their PL spectra in THF–water mixtures are measured. NpDMS and NpMPS show greatly intensified PL emissions at high water fractions (Fig. 1B and Fig. S1A, ESI†), and their Φ_F values are increased accordingly (Table 1). But only

slight enhancement in emission intensities (Fig. 1C and Fig. S1B, ESI†) and Φ_F values are observed for AnDMS and AnMPS under the same conditions. Their short-wavelength emissions vanished, and long-wavelength emissions became dominant in aqueous media, accompanied by a strong red shift. Since these siloles are insoluble in water, the silole molecules must have aggregated in the mixture with high water fractions. Thus, the IMR process is restricted and the synergistic effect among segments in the backbone is strengthened as well, accounting for the enhanced long-wavelength emission.[6] On the other side, the planar and π-extended An is prone to close π–π stacking in the condensed phase, which induces strong intermolecular interactions, and hence, gives rise to red-shifted PL emission. Since Np is smaller than An in volume, intermolecular interactions are mitigated when NpDMS and NpMPS aggregate, furnishing close emission peaks in both solution and aggregated states.

The PL emission peaks of NpDMS and NpMPS in solid films are located at 500 and 515 nm, respectively, being close to those in solutions (Fig. S2, ESI†). The Φ_F values of the films of NpDMS and NpMPS are 48 and 37%, respectively, which are about 22- and 15-fold higher than those in solutions because of the restriction of the IMR process by the spatial constraint. The films of AnDMS and AnMPS emit at 533 and 559 nm, respectively, and their Φ_F values (16% and 14%) in films are barely increased relative to those in solutions. Although the IMR process is deactivated in the aggregated state and the radiative decay of the excited state is promoted, the quenching effect of strong intermolecular interactions stemmed from flat An segments is activated in the aggregated state. Hence, AnDMS and AnMPS show lower emission efficiencies and larger red shifts than NpDMS and NpMPS in solid films.

To gain a deep insight into the structure–property relationship, DFT/TD-DFT calculations on DMTPS, NpDMS and AnDMS were carried out using a B3LYP/6-31G(d,p) basis set. The electronic clouds of HOMOs and LUMOs are mainly located on the molecular backbones comprised of silole rings plus Np or An segments (Fig. 2). The orbitals from the Phs at the 3,4-positions contribute much less. In the ground state (S_0), the dihedral angles between silole rings and Np are 47.24°, and those between silole rings and An are 46.67° (Table 2). DMTPS, however, shows much larger dihedral angles (64.55 and 64.58°) between silole rings and Phs at the 2,5-positions. This indicates that Np and An conjugate better
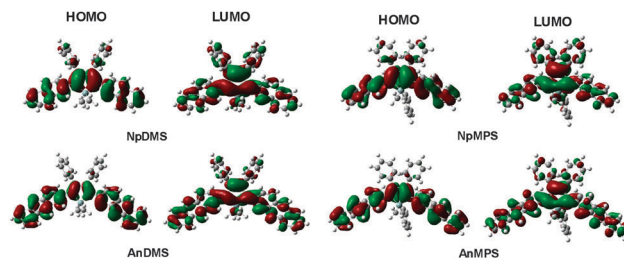

Fig. 2 Optimized molecular structures and molecular orbital amplitude plots of HOMOs and LUMOs of siloles substituted with Np and An.

Table 2 Selected dihedral angles (in deg) of the S_0 and S_1 for isolated DMTPS, NpDMS and AnDMS

	DMTPS			NpDMS			AnDMS		
	S_0	S_1	$\Delta(S_1-S_0)$	S_0	S_1	$\Delta(S_1-S_0)$	S_0	S_1	$\Delta(S_1-S_0)$
Si–C2–C8–C9	64.55	34.58	−29.97	47.24	32.20	−15.04	46.67	31.60	−15.07
Si–C5–C6–C7	64.58	34.58	−30.00	47.24	32.21	−15.03	46.67	31.60	−15.07
C4–C3–C10–C11	49.77	50.65	0.88	57.81	56.53	−1.28	57.30	59.32	2.02
C3–C4–C12–C13	49.79	50.64	0.85	57.81	56.53	−1.28	57.32	59.32	2.00

with silole rings than Phs do in DMTPS, accounting for the red-shifted absorption of siloles bearing Np and An. In the excited state (S_1), most of the geometrical parameters undergo slight modifications (Table S1, ESI†) except for the dihedral angles (Si–C2–C8–C9 and Si–C5–C6–C7) between silole rings and aromatic groups at the 2,5-positions (Table 2). The dihedral angles are reduced to 34.58, 32.20 and 31.60° in DMTPS, NpDMS and AnDMS, respectively. The changes in dihedral angles from S_0 to S_1 are ∼15° for NpDMS and AnDMS, being half of that for DMTPS (∼30°). The rotational barrier for Np is slightly smaller than that for An, but is much larger than that for Ph in DMTPS (Fig. 3). These results reveal that NpDMS and AnDMS are more rigid than DMTPS, owing to better conjugation, and possibly, higher molecular weights of Np and An than Ph. The reorganization energies in S_1 of AnDMS (2258 cm^{-1}) and NpDMS (3387 cm^{-1}) are much smaller than that of DMTPS (4920 cm^{-1}), implying less nonradiative energy loss by structural relaxation from S_1 to S_0.[8]

The excited state decays of DMTPS, NpDMS and AnDMS are also calculated. According to quantum chemical calculations, Φ_F can be expressed as $\Phi_F = k_r/(k_r + k_{nr} + k_{isc})$, where k_r and k_{nr} are the radiative and nonradiative decay rates, respectively, and k_{isc} is the intersystem crossing rate from the singlet state to a triplet one. Since the spin–orbital coupling constant between S_1 and the lowest triplet excited state (T_1) in these pure organic molecules is very small, the intersystem crossing process from S_1 to T_1 is negligible.[5b,8] Thereby, Φ_F is simplified as $\Phi_F = k_r/(k_r + k_{nr})$. The k_r can be evaluated through the Einstein spontaneous emission relationship which can be cast into a simple working formula $k_r = fE^2/1.499$, where f is the

oscillator strength of emission, and E is the transition energy of emission in cm^{-1}.[9] The calculated data of f and E are shown in Table S1 (ESI†). The k_r of AnDMS is 1.44×10^8 s^{-1}, while that of NpDMS is 1.09×10^8 s^{-1}. In addition, AnDMS has smaller reorganization energy, and thus, smaller k_{nr}. So, the larger k_r and the smaller k_{nr} of AnDMS determine its higher Φ_F in solutions. The k_r of DMTPS (0.94×10^8 s^{-1}) is slightly smaller than that of NpDMS, but its k_{nr} is much larger, which causes its extremely low Φ_F value in solutions.

In summary, a series of new siloles substituted with PAHs are synthesized and characterized. The PL emissions of siloles in solutions are improved by conjugation elongation of the substituents. The emission quenching by the IMR process is compensated by good conjugation of the molecule and thus, the AIE effect is weakened, demonstrating that the IMR process and conjugation compete against each other for determining the emission behavior. On the other side, the PAHs may induce strong intermolecular interactions in the aggregated state, which undermines the solid-state emission efficiency. These results are helpful for the understanding of the interesting AIE phenomenon and expounding why most π-conjugated chromophores are not AIE-active, and also provide useful information for the further design of luminescent materials. More comprehensive studies on the siloles substituted with PAHs are in progress.

References

1 Y. Hong, J. W. Y. Lam and B. Z. Tang, *Chem. Soc. Rev.*, 2011, **40**, 5361.
2 (a) A. J. Boydston and B. L. Pagenkopf, *Angew. Chem., Int. Ed.*, 2004, **43**, 6336; (b) M. M. Sartin, A. J. Boydston, B. L. Pagenkopf and A. J. Bard, *J. Am. Chem. Soc.*, 2006, **128**, 10163; (c) X. Zhan, S. Barlow and S. R. Marder, *Chem. Commun.*, 2009, 1948; (d) X. Du and Z. Y. Wang, *Chem. Commun.*, 2011, **47**, 4276; (e) S. Yamaguchi, T. Endo, M. Uchida, T. Izumizawa, K. Furukawa and K. Tamao, *Chem.–Eur. J.*, 2000, **6**, 1683; (f) S. Yamaguchi, R. Z. Jin and K. Tamao, *J. Organomet. Chem.*, 1998, **559**, 73; (g) Z. Li, Y. Dong, J. W. Y. Lam, J. Sun, A. Qin, M. Häußler, Y. Dong, H. H. Y. Sung, I. D. Williams, H. S. Kwok and B. Z. Tang, *Adv. Funct. Mater.*, 2009, **19**, 905.
3 (a) Z. Zhao, Z. Wang, P. Lu, C. Y. K. Chan, D. Liu, J. W. Y. Lam, H. H. Y. Sung, I. D. Williams, Y. Ma and B. Z. Tang, *Angew. Chem., Int. Ed.*, 2009, **48**, 7608; (b) J. Zhou, B. He, B. Chen, P. Lu, H. H. Y. Sung, I. D. Williams, A. Qin, H. Qiu, Z. Zhao and B. Z. Tang, *Dyes Pigm.*, 2013, **99**, 520; (c) E. Zhao, J. W. Y. Lam, Y. Hong, J. Liu, Q. Peng, J. Hao, H. H. Y. Sung, I. D. Williams and B. Z. Tang, *J. Mater. Chem. C*, 2013,
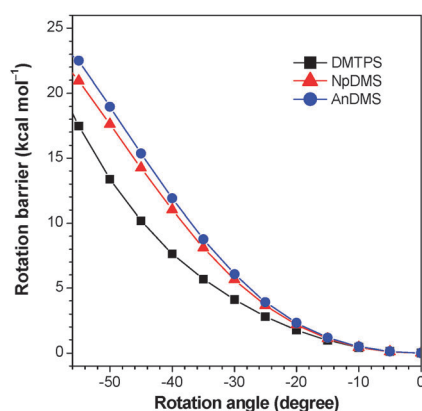

Fig. 3 Rotational energy barrier as a function of the rotational angle (Si–C2–C8–C9) in the ground state for isolated DMTPS, NpDMS and AnDMS.

1, 5661; (*d*) T. Jiang, Y. Jiang, W. Qin, S. Chen, Y. Lu, J. W. Y. Lam, B. He, P. Lu, H. H. Y. Sung, I. D. Williams, H. S. Kwok, Z. Zhao, H. Qiu and B. Z. Tang, *J. Mater. Chem.*, 2012, **22**, 20266.

4 (*a*) Z. Li, Y. Dong, B. Mi, Y. Tang, M. Häussler, H. Tong, Y. Dong, J. W. Y. Lam, Y. Ren, H. H. Y. Sun, K. S. Wong, P. Gao, I. D. Williams, H. S. Kwok and B. Z. Tang, *J. Phys. Chem. B*, 2005, **109**, 10061; (*b*) Z. Zhao, J. W. Y. Lam, C. Y. K. Chan, S. Chen, J. Liu, P. Lu, M. Rodriguez, J.-L. Maldonado, G. Ramos-Ortiz, H. H. Y. Sung, I. D. Williams, H. Su, K. S. Wong, Y. Ma, H. S. Kwok, H. Qiu and B. Z. Tang, *Adv. Mater.*, 2011, **23**, 5430; (*c*) Z. Zhao, B. He, H. Nie, B. Chen, P. Lu, A. Qin and B. Z. Tang, *Chem. Commun.*, 2014, **50**, 1131.

5 (*a*) J. Chen, C. C. W. Law, J. W. Y. Lam, Y. Dong, S. M. F. Lo, I. D. Williams, D. Zhu and B. Z. Tang, *Chem. Mater.*, 2003, **15**, 1535; (*b*) G. Yu, S. Yin, Y. Liu, J. Chen, X. Xu, X. Sun, D. Ma, X. Zhan, Q. Peng, Z. Shuai, B. Z. Tang, D. Zhu, W. Fang and Y. Luo, *J. Am. Chem. Soc.*, 2005, **127**, 6335.

6 (*a*) Z. Zhao, P. Lu, J. W. Y. Lam, Z. Wang, C. Y. K. Chan, H. H. Y. Sung, I. D. Williams, Y. Ma and B. Z. Tang, *Chem. Sci.*, 2011, **2**, 672; (*b*) B. Chen, Y. Jiang, L. Chen, H. Nie, B. He, P. Lu, H. H. Y. Sung, I. D. Williams, H. S. Kwok, A. Qin, Z. Zhao and B. Z. Tang, *Chem.–Eur. J.*, 2014, **20**, 1931.

7 (*a*) M. P. Aldred, C. Li, G.-F. Zhang, W.-L. Gong, A. D. Q. Li, Y. Dai, D. Ma and M.-Q. Zhu, *J. Mater. Chem.*, 2012, **22**, 7515; (*b*) B. Xu, J. He, Y. Dong, F. Chen, W. Yu and W. Tian, *Chem. Commun.*, 2011, **47**, 6602; (*c*) B. Xu, Z. Chi, H. Li, X. Zhang, X. Li, S. Liu, Y. Zhang and J. Xu, *J. Phys. Chem. C*, 2011, **115**, 17574.

8 (*a*) Q. Wu, Q. Peng, Y. Niu, X. Gao and Z. Shuai, *J. Phys. Chem. A*, 2012, **116**, 3881; (*b*) S. Yin, Q. Peng, Z. Shuai, W. Fang, Y.-H. Wang and Y. Luo, *Phys. Rev. B*, 2006, **73**, 205409.

9 (*a*) V. Lukes, A. Aquino and H. Lischka, *J. Phys. Chem. A*, 2005, **109**, 10232; (*b*) X. Zhang, L. Chi, S. Ji, Y. Wu, P. Song, K. Han, H. Guo, T. D. James and J. Zhao, *J. Am. Chem. Soc.*, 2009, **131**, 17452.